Smooth Vertical Surface Climbing with Directional Adhesion

Sangbae Kim, Matthew Spenko, Salomon Trujillo, Barrett Heyneman, Daniel Santos, Mark R. Cutkosky
Center for Design Research
Stanford University
Stanford, CA 94305-2232, USA
contact: sangbae@stanford.edu

***Abstract*— Stickybot is a bio-inspired robot that climbs smooth vertical surfaces such as glass, plastic and ceramic tile at 4 cm/s. The robot employs several design principles adapted from the gecko including a hierarchy of compliant structures, directional adhesion, and control of tangential contact forces to achieve control of adhesion. We describe the design and fabrication methods used to created under-actuated, multi-material structures that conform to surfaces over a range of length scales from centimeters to micrometers. At the finest scale, the undersides of Stickybot's toes are covered with arrays of small, angled polymer stalks. Like the directional adhesive structures used by geckos, they readily adhere when pulled tangentially from the tips of the toes toward the ankles; when pulled in the opposite direction, they release. Working in combination with the compliant structures and directional adhesion is a force control strategy that balances forces among the feet and promotes smooth attachment and detachment of the toes.** [1]

I. Introduction

Mobile robots that can climb and maneuver on vertical surfaces are useful for inspection, surveillance, and disaster relief applications. Previous robots capable of climbing exterior building surfaces such as stucco and brick have utilized microspines similar to those found on insects [1], [25] or a controlled vortex that creates negative aerodynamic lift [28]. Smooth vertical surfaces have been climbed using suction [21], [34], magnets [7], [30], and pressure-sensitive adhesives (PSAs), such as tape [12], [27]. PSAs exhibit high adhesion on smooth surfaces but foul easily and require relatively high forces for attachment and detachment. Some researchers have circumvented this problem by using spoked-wheel designs that allow the detachment force at a receding point of contact to provide the necessary attachment force at the next [12]. Wet adhesive materials have also been employed, drawing inspiration from tree frogs and snails [9]. All of these solutions have been successful, but are limited in their range of surfaces. To develop a robot capable of climbing a wide variety of materials, we have taken design principles adapted from geckos. The result is Stickybot (Fig. 1), a robot that climbs glass and other smooth surfaces using directional adhesive pads on its toes.

Geckos are arguably Nature's most agile smooth surface climbers. They can run at over 1 m/s, in any direction, over wet and dry surfaces of varying roughness and of almost any material, with a few exceptions like graphite and Teflon [2]. The gecko's prowess is due to a combination of "design features" that work together to permit rapid, smooth locomotion. Foremost among these features is hierarchical compliance, which helps the gecko conform to rough and undulating surfaces over multiple length scales. The result of this conformability is that the gecko achieves intimate contact with surfaces so that van der Waals forces produce sufficient adhesion for climbing [2].

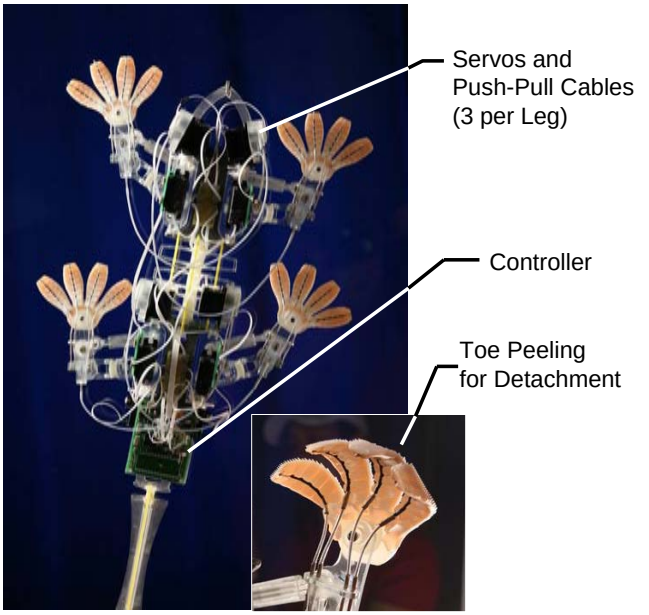

Fig. 1. Left: Stickybot, a new bio-inspired robot capable of climbing smooth surfaces. Inset: detail of toes curling to facilitate detachment.

The gecko's adhesion is also directional. This characteristic allows the gecko to adhere with negligible preload in the normal direction and to detach with very little pull-off force, an effect that is enhanced by peeling the toes in "digital hyperextension" [3].

A consequence of the gecko's directional adhesion is that it must control the orientation of its feet when ascending or descending. In addition, the gecko controls the tangential contact forces to achieve smooth climbing with minimal pull-off forces [4].

[1] Some material in this paper has been adapted from two papers, [20], [24], presented at IEEE ICRA2007.

In the following sections, we examine hierarchical compliance, directional adhesion and force control for climbing in more detail and describe how they are implemented in Stickybot. We also provide details of the design and fabrication of Stickybot's feet equipped with arrays of directional polymer stalks (DPS). We present the results of experiments to confirm the DPS directional behavior and describe the controller used to ensure that they are loaded appropriately. We also present a comparison of attachment and detachment forces for Stickybot climbing with directional versus non-directional adhesives, illustrating the advantages of the former. We conclude with a discussion of some of the limitations of the current Stickybot technology and plans to overcome them for faster, more robust and more dirt-tolerant climbing in the future.

II. Adhesion and Compliance

When two surfaces are brought together, adhesion is created via van der Waals forces. Since van der Waals forces scale as $1/d^3$ where d is the local separation between two flat surfaces, it is critical for the surfaces to be within an order of hundreds of nanometers of each other. Pressure-sensitive adhesives (PSAs) accomplish this with a soft layer that flows and conforms to the surface, thus maximizing the contact area. PSAs can provide sufficient adhesion levels for a robot to climb a wall [12], [27], but they have several disadvantages compared to the hierarchical compliant structures used by geckos. To adhere to rough surfaces an additional layer of conformability is usually required, which is why adhesive tapes for brick and concrete often have a backing layer of soft foam. Substantial preloads in the normal direction are required to achieve adhesion and large forces are also required for detachment, leading to inefficient climbing. In addition, PSAs quickly become contaminated with dirt and lose their stickiness.

To overcome the limitations of PSAs, there has been recent interest in creating synthetic "dry" or "self-cleaning" adhesives that do not foul over time. These adhesives use stiff, initially non-sticky bulk materials in combination with microstructured geometries to conform to surfaces. Figure 2 shows some adhesive solutions ordered in terms of feature size, shape sensitivity and effective modulus. For a material to be considered tacky, its effective modulus must be less than 100kPa [2], [10], [5]. This "tack criterion" comes from the need to conform intimately to a surface in order for van der Waals forces to become significant. The gecko conforms to surfaces despite having a relatively high bulk material stiffness ($\approx$ 2GPa for β-keratin) [2] by using a hierarchy of microstructures consisting of lamellae, setae, and spatulae. This hierarchical geometry lowers the effective stiffness to make the system function like a tacky material.

Several types of synthetic dry adhesives have been manufactured, including arrays of vertically oriented multiwall carbon nanotubes [32], [33] and polymer fibers [14], [18], [22], [26]. These adhesives use stiff, hydrophobic materials

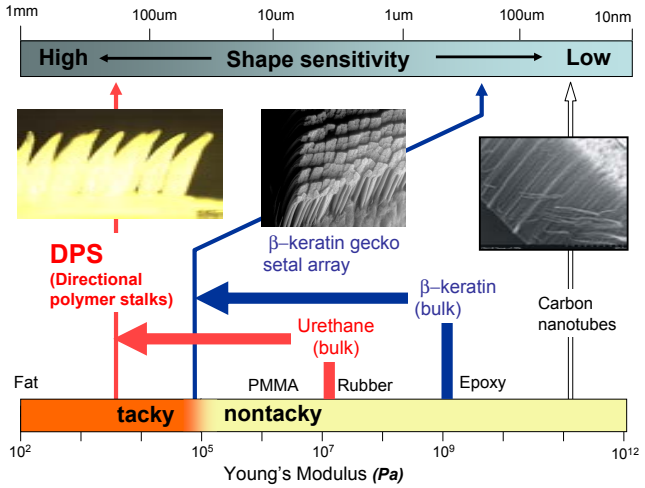

Fig. 2. Shape sensitivity of different structures and modulus of elasticity of various materials. Microstrucutred geometries can lower the overall stiffness of bulk materials so that they become tacky. This principle allows geckos to use β-keratin for their adhesive structures.

and have achieved useful levels of adhesion, but only with careful surface preparation and high normal preloads.

An alternative method to creating adhesives is to start with a somewhat softer material on the order of 300kPa to 3MPa. These materials can employ larger feature sizes and still conform to surfaces because they are softer to begin with. Unlike dry adhesives, these materials will attract dirt; however, in contrast to PSAs, they can be cleaned and reused. One such example is a microstructured elastomer tape [11], [23].

In addition to stiffness, the size and shape of the contacting elements is important in sustaining adhesion [13], [14], [19], [31]. For extremely small elements such as carbon nanotubes, the shape sensitivity (Fig. 2 top) is low but for softer materials and larger features ($O(100\mu\text{m})$) tip geometry dramatically affects adhesion. At these sizes, the optimal tip geometry, where stress is uniformly distributed along the contact area, has a theoretical pulloff force of more than 50-100 times that of a poor tip geometry[13]. Recent developments have included microstructured elastomeric arrays that have a flattened tip geometry, somewhat analogous to the spatulae of gecko setal stalks [14], [19], for higher pull-off forces and reduced sensitivity to surface contamination.

A. Hierarchical Conformability in the Gecko

For climbing rough surfaces such as cave walls and trees, many levels of conformability are required. In the gecko, the flex of the body and limbs allows for conformation at the centimeter scale. The body presses flat against curved surfaces to reduce the pull-in forces needed to prevent pitching back. At the scale of a several millimeters, the toes conform independently to local surface variations. The bottom surfaces of toes are covered with lamellae that conform

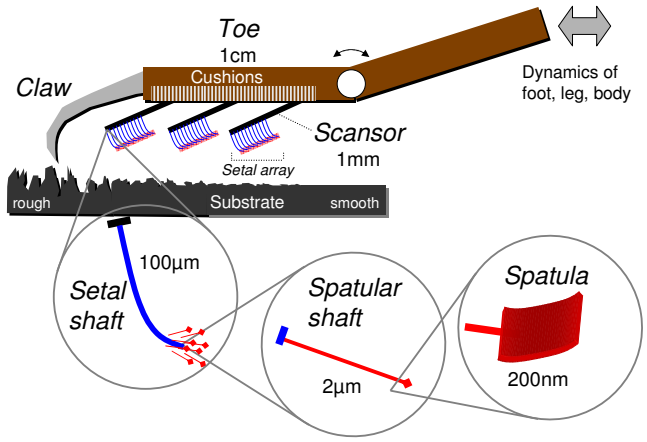

Fig. 3. Hierarchy of compliant structures in the gecko for conforming at many length scales. (From [5], reprinted with the permission of K. Autumn).

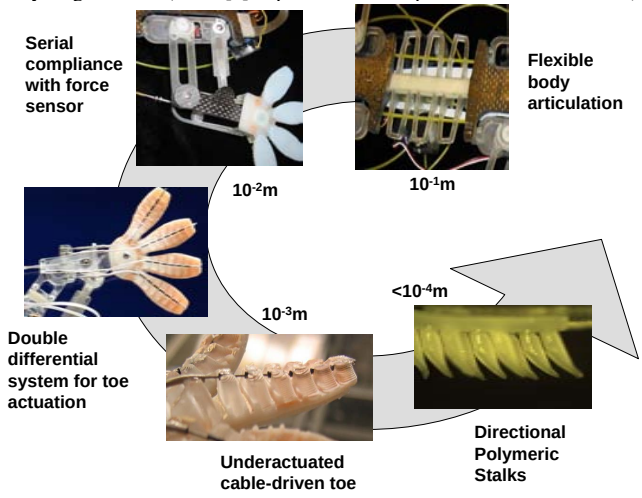

Fig. 4. The elements of Stickybot's hierarchical compliance over a range of length scales.

at the millimeter scale. The lamellae consist of arrays of setal stalks, as shown in Figs. 2 and 3. The consequence of the gecko's hierarchical system of compliances is that it can achieve levels of adhesion of over 500 KPa on a wide variety of surfaces from glass to rough rock and can support its entire weight in shear from just one toe [6].

B. Hierarchical Conformability in Stickybot

Stickybot uses an analogous, albeit much less sophisticated, hierarchy of conformable structures to climb a variety of smooth surfaces (Fig. 4). At the body level, Stickybot has 12 servo-motors and 38 degrees of freedom, making it highly underactuated. The structures of the torso, legs and feet are manufactured using Shape Deposition Manufacturing [29], [8] with two grades of polyurethane (Innovative Polymers: 72 Shore-DC and 20 Shore-A hardness). The upper and lower torso and forelimbs are reinforced with carbon fiber, making them the strongest and stiffest components. The middle of the torso is designed as a compromise between sufficient compliance to conform to surfaces and sufficient stiffness so that normal forces of approximately +/-1 N can be applied at the feet without excessive body torsion.

The feet of Stickybot consist of four segmented toes molded with two grades of polyurethane that sandwich a thin polyester fabric (Fig. 5). The fabric flexes easily, but is relatively inextensible so that it transmits shear stresses across the surface of the foot to avoid the buildup of stress concentrations, and subsequent peeling, at the proximal regions of the toes.

The bending of the toes allows them to conform to gently curved surfaces ($r \geq 5$ cm, where r is the radius of curvature) and to peel backward in a motion that approximates the digital hyperextension that geckos use to facilitate detachment. The action is created using a servomotor connected via push-pull cables in sleeves, attached to a rocker-bogie linkage located at the foot (Fig. 6).

The profile of the steel cable running along the topside of each toe is calculated to achieve a uniform stress distribution when the toes are deployed on a flat surface (Fig. 7). Assuming an approximately uniform toe width, the sum of the forces in the y direction is given as:

$$T \sin\theta - T \sin(\theta + \delta\theta) + F_n = 0 \tag{1}$$

where T is the force acting along the cable, θ is the angle of the cable with respect to the horizontal, and F_n is the normal force acting on the bottom of the toe. To ensure uniform attachment of the foot, a constant pressure on the bottom of the toe is desired:

$$\frac{T(\sin(\theta + d\theta) - \sin\theta)}{dx} = \frac{F_n}{dx} = \sigma \tag{2}$$

Expanding the term $\sin(\theta + d\theta)$ and assuming that $d\theta$ is small such that $\cos d\theta = 1$ and $\sin d\theta = d\theta$ yields:

$$\cos\theta d\theta = \frac{\sigma}{T} dx \tag{3}$$

Integrating both sides and solving for θ gives:

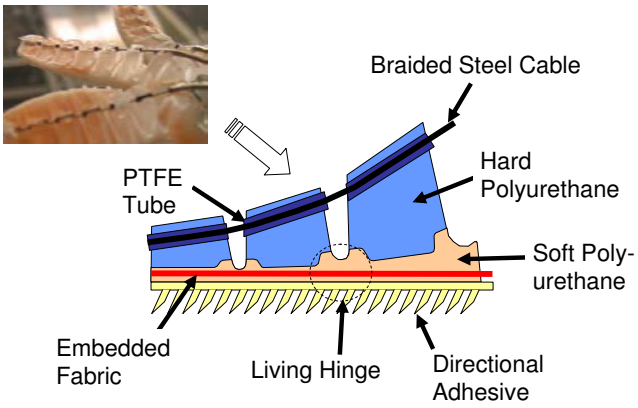

Fig. 5. Schematic of cross section view of Stickybot toe fabricated via Shape Deposition Manufacturing.

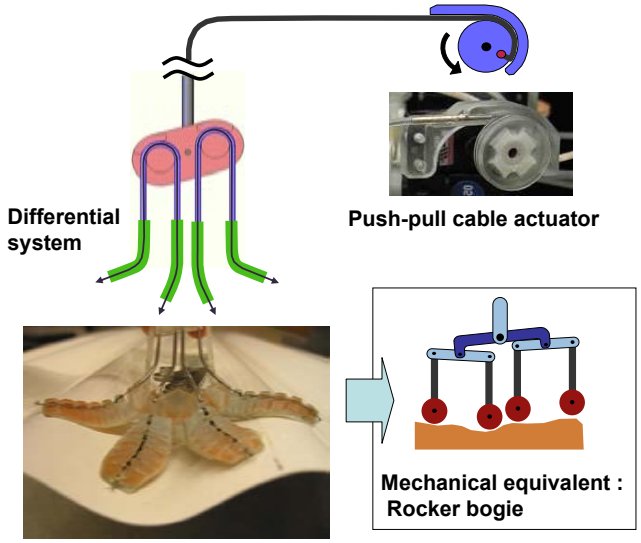

Fig. 6. Two stage differential system actuated by a single push pull actuator. It facilitates conformation on uneven surfaces and distributes the contact forces among four toes.

$$\theta = \arcsin\left(\frac{\sigma x}{T}\right) \tag{4}$$

The slope of the cable profile is thus:

$$\frac{dy}{dx} = \tan\left(\arcsin\left(\frac{\sigma x}{T}\right)\right) \tag{5}$$

Integrating with respect to x yields the profile of the cable:

$$y\left(x\right) = -\frac{T}{\sigma}\sqrt{1-\left(\frac{\sigma x}{T}\right)^2} \tag{6}$$

which is simply a circular arc with radius T/σ.

At the the scale of hundreds of micrometers, Stickybot conforms to the surface with synthetic adhesive patches (Fig. 5). Currently, the best results have been obtained using arrays of small, asymmetric features comprised of polyurethane with a modulus of elasticity of $300kPA$ (Fig. 8). A detailed description of the hairs is given in the following section including the manufacturing process and importance of the anisotropic geometry. We are currently investigating alternate manufacturing methods that will yield finer feature sizes and comparable adhesion with stiffer materials.

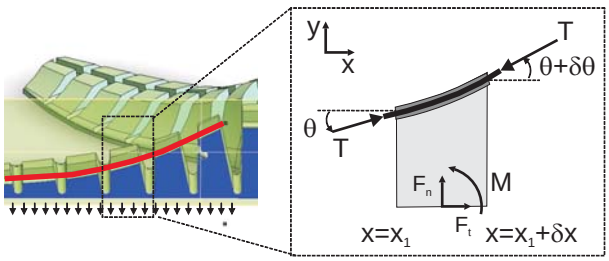

Fig. 7. Details of nomenclature used to calculate cable profile of the toes.

III. Directional Friction and Adhesion

As discussed in [3], the gecko's toe structures are only adhesive when loaded in a particular direction. Moreover, the amount of adhesion sustained is a direct function of the applied tangential load. In other words, the gecko can control adhesion by controlling tangential forces. The anisotropic adhesion results from the gecko's lamellae, setae, and spatulae all being angled instead of aligned vertically. Only by pulling in the proper direction does the gecko align its microstructures to make intimate contact with the surface.

Directional Polymer Stalks (DPS) were designed and manufactured to create an adhesive that is also directional like the gecko's system. DPS are made out of a soft polyurethane (Innovative Polymers, IE-20 AH Polyurethane, 20 Shore-A hardness, $E \approx 300\text{kPa}$) and are shown in Fig. 8. Because of the complexity of the gecko hierarchical system, the initial bulk material can be quite stiff; however, DPS begin with a fairly soft material that is already marginally sticky. Geometric properties were determined empirically, drawing inspiration from the shapes of gecko setae. Not having fine distal structures like spatulae, the DPS need low stiffness tips in order to make contact without high normal preload. The sharp and thin ($< 30\mu\text{m}$) tip shape of DPS is designed to create a softer effective stiffness when pulled parallel to the angle of inclination.

The overall mold to create DPS consists of three parts. The middle mold is made out of Delrin, which has good machinability and relatively low surface energy so that it does not bond to the curing polymer. First, V-shaped grooves are made in a $1.6\text{mm} - \text{thick}$ Delrin sheet as shown in Figure 9. Before the drilling process, the top mold is fabricated by casting silicon rubber on the middle mold. On the $45°$ slanted surfaces and at a $20°$ tilted angle, $380\mu\text{m}$ holes are made in a hexagonal pattern, maximizing stalk density. The bottom mold is made out of a wax that has the Stickybot toe pattern.

Before pouring polymer, the middle and bottom mold are assembled. After pouring polymer on this assembly, the top mold is applied, squeezing out any excess material.

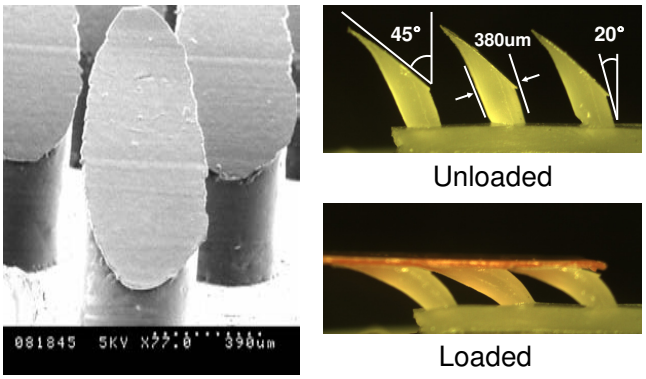

Fig. 8. Anisotropic hairs comprised of 20 Shore-A polyurethane. Hairs measure 380 μm in diameter at the base. The base angle is $20°$ and the tip angle is $45°$.

The DPS array is released after curing by disassembling the molds. An alternative manufacturing method has also been used to create softer and smoother tip surfaces. Instead of using a top mold, excess polymer is simply wiped off of the 45° slanted surfaces and the polymer is exposed to air during curing. Exposure to atmospheric moisture during the cure creates softer and stickier tips. However, this method is less desirable because it is difficult to control the moisture-induced softening. The wiping process is also labor-intensive.

The DPS were tested using a three-axis positioning stage and a six-axis (ATI Gamma Transducer) load cell in order to study their adhesive characteristics. The stage was able to control motion of the DPS in the normal, tangential (fore-aft), and lateral direction of the DPS (Fig. 9). The load cell was used to measure the pulloff force when the patches detached from a glass substrate. Patches of the DPS were brought into contact, preloaded, and then pulled away from the glass at different departure angles. When the patches are pulled in directions along the stalk-angle they exhibit moderate amounts of adhesion. When pulling in the opposite directions, adhesion disappears and Columb friction is observed.

Data from the tests are shown in Fig. 10 for the normal-tangential plane, plotted in force-space. Figure 10 also shows the frictional adhesion model, which has been proposed in [3] as a simple way to describe the macroscopic gecko adhesion system, and the well-known isotropic Johnson-Kendall-Roberts (JKR) model for elastomers [15]. The frictional adhesion model has been scaled to fit the data from the DPS patches and the JKR model has been scaled for comparison purposes. Mathematically, the frictional adhesion model is given by:

$$\begin{array}{c} F_N \geq -\frac{1}{\mu} F_T \\ F_N \geq -\tan(\alpha^*) F_T \end{array} \quad \begin{cases} F_T < 0 \\ 0 \leq F_T \leq F_{max} \end{cases} \tag{7}$$

where α^* is the critical angle [3], μ is the coefficient of friction, F_T is tangential (shear) load, taken positive when pulling inward, and F_N is the normal force, taken positive when compressive. The limit, F_{max}, is a function of the maximum shear load that a gecko or robot can apply, the material strength, and the shear strength of the contact interface. Equation 7 shows how the maximum adhesion is directly related to the amount of tangential force present.

The curves in Fig. 10 are the respective two-dimensional limit curves for the contact, i.e., the limiting combinations of normal and tangential force that will cause the contact to fail. The DPS show behavior similar to the frictional adhesion model for the gecko and are clearly anisotropic with respect to adhesion. The DPS data also resemble data that would be obtained for peeling a sticky, elastic tape as described in the Kendall peel model [16]. In this case, although the toe patches are not peeled like a tape from one edge, the individual stalk tips do peel like tape of tapering thickness. However, the behavior of the DPS arrays at the origin (approaching zero tangential force and normal force) is closer to that of the frictional adhesion model than the Kendall tape peeling model.

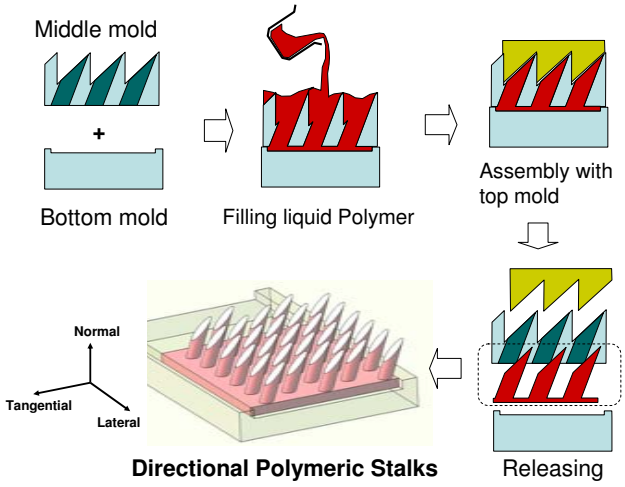

Fig. 9. Molding process used to fabricate anisotropic patches. Mold is manufactured out of hard wax and then filled with liquid urethane polymer. A cap eliminates contact with air and creates final tip geometry.

Figure 11 shows the corresponding pulloff force data for the DPS in the normal-lateral plane. Not surprisingly, the DPS show symmetric behavior when pulled in the positive or negative lateral direction. The amount of adhesion depends on the amount of tangential loading that is also present. Taken together, the two data sets in Figs. 10 and 11 represent slices of a convex three-dimensional limit surface in force space. Forces within the limit surface are safe; forces outside the surface will cause failure through sliding or detachment.

A consequence of the directional behavior of the DPS array is that the amount of adhesion can be controlled by changing the tangential force. To increase the available adhesion, the robot can pull harder in the tangential direction. Conversely, to facilitate smooth detachment the robot can unload the foot in the tangential direction, approaching the origin in Fig. 10. In contrast, an isotropic elastic material described by the JKR model is difficult to detach smoothly because maximum adhesion is present when the tangential force is zero.

More generally, the directional adhesion in geckos and Stickybot requires different force control strategies than isotropic adhesion. A simple two-dimensional model can be used to illustrate the difference. Figure 12 shows schematically the optimal tangential forces at the front and rear feet of a planar gecko or robot perched on surfaces of various inclinations. There are three equilibrium equations in the plane and four unknowns, corresponding to the magnitudes of the normal and tangential forces at each foot. The remaining degree of freedom is the magnitude of the internal (compressive or tensile) force, parallel to the surface, between the front and rear feet: $F_{Int} = F_{T1} - F_{T2}$. The internal force can be adjusted to keep each contact within

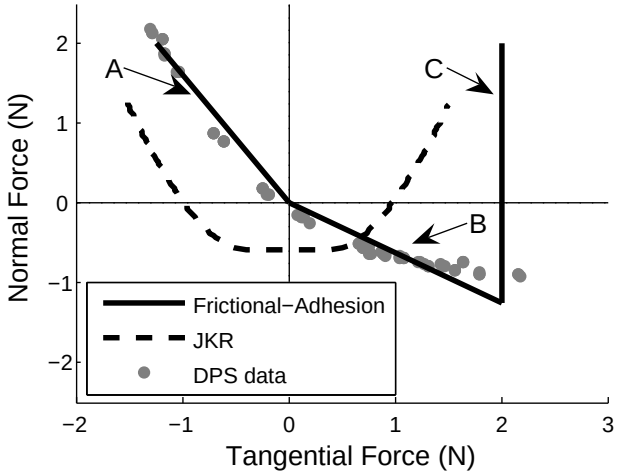

Fig. 10. Comparison of the frictional-adhesion model [3] and the Johnson-Kendall-Roberts (JKR) model [15] with pull off force data from a single toe of Stickybot's directional adhesive patches (513 stalks). (A) When dragged against the preferred direction, the directional patch exhibits friction and no adhesion. (B) When dragged in the preferred direction, the directional patch demonstrates adhesion proportional to the shear force, albeit with saturation at the highest levels (unlike gecko setae). (C) The frictional-adhesion model has an upper shear force limit. In comparison, the JKR model shows the typical behavior of an isotropic elastic material with adhesion.

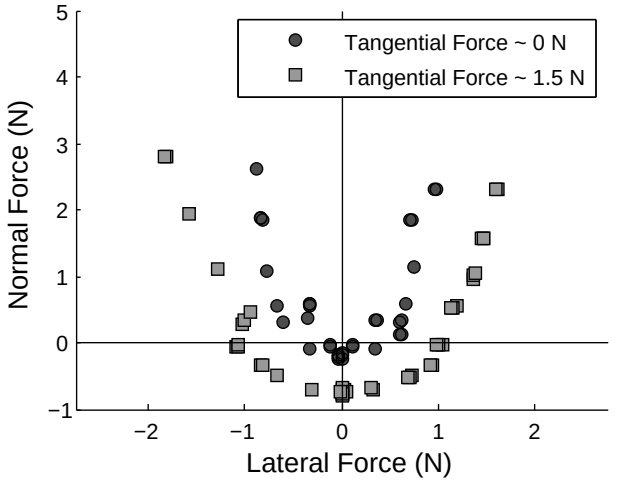

Fig. 11. Pulloff data for the DPS patches in the normal-lateral plane. Data is shown for two different levels of tangential force, approximately 0 N and 1.5 N.

its corresponding limit surface. Let $\mathbf{F_i} = [F_{Ti}, F_{Ni}]$ be the contact force at the i^{th} foot. The contact model can be defined by a parametric convex curve $\mathbf{R}(x, y)$, with points $\mathbf{F} = [F_T, F_N]$ lying inside the curve being stable contacts. The distance any particular foot is from violating a contact constraint is then:

$$d_i = \min_{x,y}(||\mathbf{F_i} - \mathbf{R}(x, y)||). \quad (8)$$

For a model with two feet in contact with the surface, the overall stability margin becomes $d = \min(d_1, d_2)$, where d_1 represents the front foot and d_2 represents the rear foot.

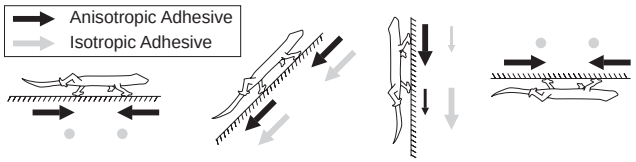

Fig. 12. Schematic of optimal tangential forces for a planar two-legged climber under isotropic versus anisotropic adhesion at different inclinations. Arrow directions and magnitudes shown in proportion to optimal tangential forces (dot represents zero tangential force).

Results of optimizing stability for the planar model using both the contact models given in Figure 10 are given in Figure 12. On vertical surfaces the front foot must generate adhesion to prevent pitch-back. The anisotropic model predicts that the front foot should bear more of the weight, since increasing tangential force increases available adhesion. The opposite is true for the isotropic model, namely that the rear foot should bear more weight because tangential forces on the front foot decrease adhesion. On inverted surfaces, the isotropic model predicts zero tangential forces since gravity is pulling along the normal, maximizing adhesion. Alternatively, the anisotropic model cannot generate adhesion without tangential forces and in this case the rear foot must be reversed and both feet must pull inward to generate tangential forces that will produce enough adhesion for stability. Interestingly, the anisotropic model also predicts the same foot reversal strategy is optimal on level ground, which would increase the maximum perturbation force that could be withstood. The predictions of the anisotropic model qualitatively match observations of geckos running on walls and ceilings and reorienting their feet as they climb in different directions [4].

IV. Distributed Force Control

A. Distributed Force Control in the Gecko

As the previous section suggests, unlike a walking or running quadruped, a climbing gecko or robot must pay continuous attention to the control of internal forces whenever its feet are in contact with the climbing surface. In the gecko, it has been observed that even at speeds of over 1 m/s, attachment and lift-off are smooth, low-force events[4]. The gecko does not need to produce decelerating contact forces while climbing, but it does need to adjust the orientation of its feet as it manuevers, to ensure that toes are always loaded in the proper direction for adhesion. On overhanging surfaces the lateral forces are high, as one would expect, and directed inward toward the center of mass. Geckos can also use their tails to affect the dynamic force balance. If the front feet lose their grip, the tail immediately presses against the wall and the rear legs provide the necessary pull-in force [4].

B. Distributed Force Control in Stickybot

To achieve smooth engagement and disengagement and control of internal forces, Stickybot employs force feed-

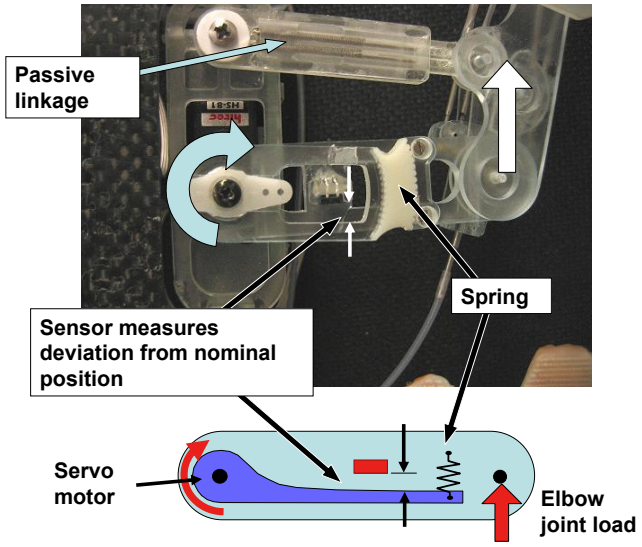

Fig. 13. Tangential force sensor measuring deviation of serial compliance at shoulder joint.

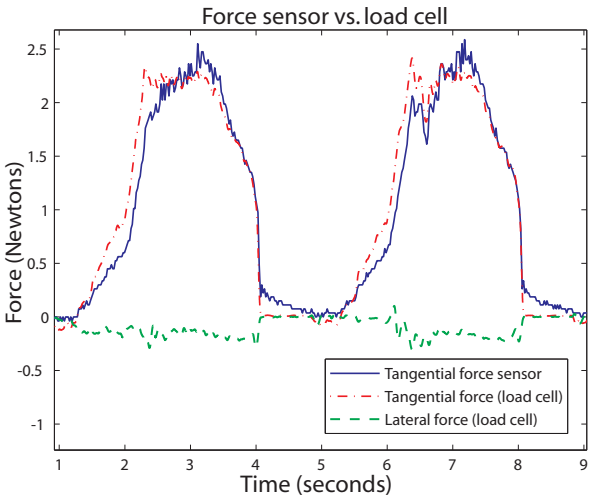

Fig. 14. Unfiltered tangential force sensor readings compared to tangential and lateral forces measured using a force plate mounted to a load cell.

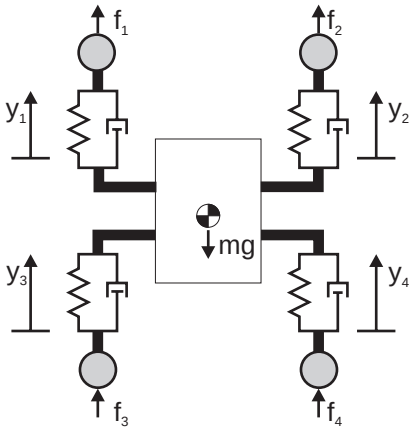

Fig. 15. Schematic used to generate values for the grasp matrix

back in the tangential (fore-aft) direction, coupled with a grasp-space stiffness controller. The control is implemented in hardware using a single master microcontroller (PIC18F4520) and four slave microcontrollers (PIC12F683) connected using an I^2C bus. The master microcontroller runs the control code and outputs the twelve pulse-width-modulated signals to independently control each of Stickybot's servos (two servos for each leg and an additional servo for flexing the toes). Each slave microcontroller reads and digitizes the analog force sensor data from a single leg and transmits that digital data to the master over the I^2C bus.

C. Force Sensors

Stickybot's force sensors are located on its shoulder joints (Fig. 13) and measure the deflection of an elastomeric spring via a ratiometric Hall effect sensor (Honeywell: SS495A). The Hall effect sensor outputs an analog voltage as a function of its position between two anti-aligned magnets. This analog voltage is digitized and run through a software low-pass filter at 50 Hz.

The mapping from tangential force to sensor output is affected by the nonlinearity of the viscoelastic spring and the Hall effect sensors' output as a function of displacement. In addition, as Stickybot's limbs rotate, both tangential and lateral forces can contribute to the displacement in the compliant element. However, due to the computation and space limitations of Stickybot's master microcontroller, the control law simply models the mapping as a linearization about zero force and zero displacement. Figure 14 provides a comparison of the tangential force sensor output with the tangential and lateral contact forces for two successive contact periods, as measured by a vertical force plate mounted to the same six-axis load cell used in the previously described pull-off experiments. The figure shows that the tangential force sensor tracks the tangential forces relatively closely and that the lateral forces are small because, unlike the gecko, Stickybot cannot reorient its feet.

D. Force Controller

When multiple limbs are in contact with the climbing surface, Stickybot's controller must consider how to coordinate them while continuing its vertical motion. This presents two different and sometimes contradictory goals: force balancing and leg positioning. In order to handle this tradeoff, Stickybot's controller implements a grasp-space stiffness controller [17]. Since Stickybot uses servomotors that only accept position commands, the stiffness control law is given as:

$$\mathbf{y_{cmd}}(t) = \mathbf{y_{ff}}(\phi(t)) + \mathbf{C}(\mathbf{f_s}(t) - \mathbf{f_d}(\phi(t))) \quad (9)$$

where $\mathbf{y_{cmd}}$ is the vector of stroke servo commanded positions, $\mathbf{y_{ff}}$ is the feed forward position command (open

loop gait), $\mathbf{C}$ is the compliance matrix, $\mathbf{f_s}$ is the vector of force sensor readings, $\mathbf{f_d}$ is the vector of desired tangential forces, and $\phi(t)$ is a function that maps from continuous time into periodic gait phase. While a diagonal compliance matrix, $\mathbf{C}$, would result in independent leg control, during stance it is defined as:

$$\mathbf{C} = \mathbf{G}^{-1}\mathbf{C_0}\mathbf{G} \tag{10}$$

where $\mathbf{C_0} \neq \mathbf{I}$ is a diagonal gain matrix and $\mathbf{G}$ is the grasp matrix given as:

$$\mathbf{G} = \frac{1}{2}\begin{bmatrix} 1 & 1 & 1 & 1 \\ 1 & -1 & 1 & -1 \\ 1 & 1 & -1 & -1 \\ 1 & -1 & -1 & 1 \end{bmatrix} \tag{11}$$

The grasp matrix is comprised of four independent "grasp modes", or ways to linearly combine the force sensor data. The first row in $\mathbf{G}$ corresponds to summing the tangential forces (Figure 15). The second row corresponds to a measure of the sum of moments about the center of mass (the difference between total tangential force on the left and right limbs). The third and fourth rows are chosen such that $\mathbf{G}$ is orthogonal, thereby leaving four independent modes of control. The chosen values for those rows correspond to fore-aft and diagonal coupling of the limbs respectively. The implementation of stiffness control in grasp space creates a framework for force distribution. By increasing the compliances of all but the total-tangential mode, the robot will evenly distribute the forces between feet and achieve force balance while remaining stiff to variations in loading.

V. Results

Stickybot is capable of climbing a variety of surfaces at $90\,\mathrm{deg}$ including glass, glossy ceramic tile, acrylic, and polished granite at speeds up to 4.0 cm/s (0.12 body-lengths/s, excluding the tail). The maximum speed of Stickybot on level ground is 24cm/s and is limited by the speed of its actuators (Table I).

Figure 16 presents typical force plate data of Stickybot climbing vertical glass. The left side shows data from the rear left foot and the right side displays data from the front right foot. Forces are in N and time in seconds. Data from two successive runs are shown to give an indication of the repeatability.

Section A (0 to 1.5 seconds) represents the preloading and flexing of the foot. There is almost no force in the lateral (X) direction during preload. The tangential force (- Y) is increasing. Although each foot would ideally engage with negligible normal force, there is a small amount of positive normal force during engagement. Weight transfer between diagonal pairs also occurs during section A.

Section B represents the ground stroke phase. There are equal and opposite forces in the X direction for the front right and rear left feet, indicating that the legs are pulling in toward the body. This helps stabilize the body and is

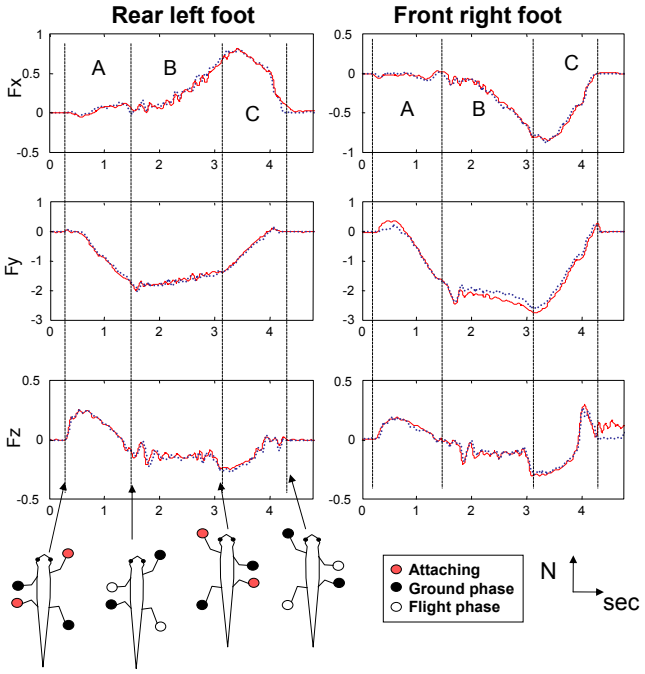

Fig. 16. Force plate data of rear left foot (left) and front right foot (right) of Stickybot climbing with a 6s period at a speed of 1.5 cm/s. Data filtered at 10Hz. Two successive runs are shown to illustrate repeatability.

similar to the lateral forces exhibited in geckos (and in contrast to the *outward* lateral forces observed in small running animals such as lizards and insects) [4]. The Y-direction shows relatively steady tangential force, and the Z-direction indicates adhesion on both the front and rear feet. Note that this differs from gecko data, in which the rear feet exhibit positive normal force [4]. This is due to the fact that Stickybot uses its tail to prevent the body from pitching back, and geckos usually use their rear feet.

In section C Stickybot releases the feet both by reducing the traction force (Y) and by peeling (utilizing digital hyperextension). Both the front and rear feet exhibit low detachment forces in the Z-direction, especially the rear foot. We note also that the transition between B and C is accompanied by a temporary increase in adhesion (-Z force) and subsequent decrease as the opposite diagonal feet come into engagement.

Figure 17 shows a comparison of the force data for climbing with directional versus isotropic adhesive elastomeric pads. In this test, the isotropic pads were composed of arrays of pillars connected by a thin outer membrane of soft polyurethane (Innovative Polymers Inc. Shore 20A) to increase the contact area on smooth surfaces. The data for three successive cycles are shown to give an estimate of cycle to cycle variability. In each case, the robot cycled a single leg through an attach/load/detach cycle using the same 6-axis load cell as in the previous tests. The other three limbs remained attached to the wall. As the plots show, the isotropic patches required a somewhat larger normal force

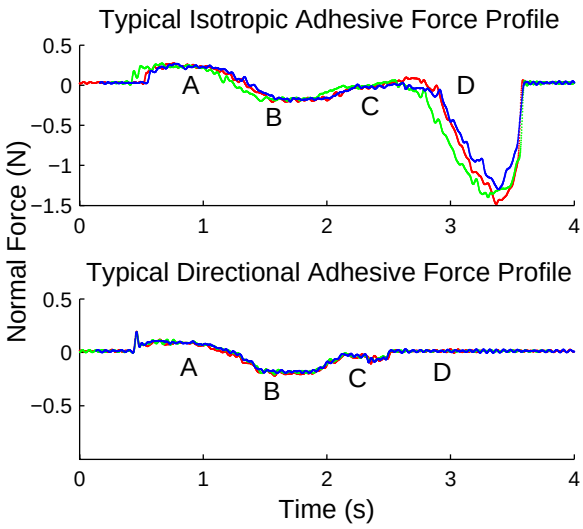

Fig. 17. Comparison of normal force profiles of anisotropic and isotropic patches on a climbing robot. Point A on the curves refers to the preloading phase of the cycle. Point B highlights when the foot is in the adhesive regime during a stroke. Points C and D are when the foot is unloaded and detached, causing large normal forces in the case of the isotropic patch.

(point (A) in the figure) to produce comparable amounts of combined tangential force and adhesion for climbing (B). The unloading step for the anisotropic patches (C) is accomplished rapidly and results in negligible detachment force as the leg is removed. In contrast, the isotropic patch requires a longer peeling phase (C) and produces a very large pull-off force as the leg is withdrawn. This large detachment force was the main limitation of of the isotropic patches, producing oscillations that frequently caused the other feet to slip.

TABLE I

PHYSICAL PARAMETERS FOR *Stickybot*

Body size	600 x 200 x 60 mm (excluding cables)
Body mass	370 g (including batteries and servo circuitry)
Maximum speed	4.0 cm/s (0.05 bodylength/s)
Servo motors	Hitec HB65 x 8 Hs81 x 4
Batteries	lithium polymer x2 (3.7 V, 480 mAh per pack)

VI. CONCLUSIONS AND FUTURE WORK

Taking cues from geckos, Stickybot uses three main principles to climb smooth surfaces. First, it employs *hierarchical compliance* that conforms at levels ranging from the micrometer to centimeter scale. Second, Stickybot takes advantage of *directional adhesion* that allows it to smoothly engage and disengage from the surface by controlling the tangential force. This prevents large disengagement forces from propagating throughout the body and allows the feet to adhere themselves to surfaces when loaded in shear. Interestingly, the motion strategy for engaging adhesives is similar to that used for microspines [1]. Third, Stickybot employs *force control* that works in conjunction with the body compliance and directional adhesive patches to control the traction forces in the feet.

Some of Stickybot's directional adhesive patches have been in continuous use for over 6 months without significant loss in performance; however, because the DPS are made from a polyurethane that degrades with time, their sharp geometric features will eventually dull and the patches will begin to lose some of their adhesive performance. As discussed in Section II, the DPS use bigger feature sizes and a relatively softer material and this prevents them from being self-cleaning. The adhesive patches require periodic cleaning to maintain enough performance to allow Stickybot to climb well. After about 3 to 4 meters of climbing, the patches need to be cleaned using tape, similar to the process of using a lint roller. Another failure associated with the DPS are that the stalk tips can fold on themselves; however, in this case, the DPS can be reconditioned via a more thorough cleaning with soap and water.

The introduction of better adhesive structures with improved hierarchical compliances will allow Stickybot to climb rougher surfaces and yield longer climbs with an increased resistance to becoming dirty. These improvements may also permit the climbing of overhanging surfaces. Other improvements include improved force control and more attention to the gait and control of internal forces. Additional sensors in the feet should allow the robot to detect when good or poor contact has been made, which will improve the reliability of climbing on varying surfaces. Additional degrees of freedom in the body should allow the robot to master vertical-horizontal transitions and other discontinuities. Once the climbing technology is understood, the ability to climb smooth surfaces will be integrated into the RiSE family of robots in an attempt to design a machine capable of climbing a wide variety of man-made and natural surfaces using a combination of adhesion and microspines [25].

ACKNOWLEDGEMENTS

We thank Jonathan Karpick, Sanjay Dastoor, and Arthur McClung for their help in circuit board fabrication, coding, and gait generation in support of Stickybot. The development of Stickybot is supported by the DARPA BioDynotics program. Matthew Spenko is supported by the Intelligence Community Postdoctoral Fellow Program and Daniel Santos was supported by the Stanford-NIH Biotechnology Training Grant.

REFERENCES

[1] A. Asbeck, S. Kim, M. Cutkosky, W. Provancher, and M. Lanzetta. Scaling hard vertical surfaces with compliant microspine arrays. *International Journal of Robotics Research*, 2006.

[2] K. Autumn. *Biological Adhesives*, volume XVII. Springer-Verlog, Berlin Heidelberg, 2006.

[3] K. Autumn, A. Dittmore, D. Santos, M. Spenko, and M. Cutkosky. Frictional adhesion: a new angle on gecko attachment. *J Exp Biol*, 209(18):3569–3579, 2006.

[4] K. Autumn, S. T. Hsieh, D. M. Dudek, J. Chen, C. Chitaphan, and R. J. Full. Dynamics of geckos running vertically. *J Exp Biol*, 209(2):260–272, 2006.

[5] K. Autumn, C. Majidi, R. E. Groff, A. Dittmore, and R. Fearing. Effective elastic modulus of isolated gecko setal arrays. *J Exp Biol*, 209(18):3558–3568, 2006.

[6] K. Autumn, M. Sitti, Y. Liang, A. Peattie, W. Hansen, S. Sponberg, T. Kenny, R. Fearing, J. Israelachvili, and R. Full. Evidence for van der waals adhesion in gecko setae. *Proc. of the National Academy of Sciences of the USA*, 99(19):12252–12256, 2002.

[7] C. Balaguer, A. Gimenez, J. Pastor, V. Padron, and C. Abderrahim. A climbing autonomous robot for inspection applications in 3d complex environments. *Robotica*, 18(3):287–297, 2000.

[8] M. Binnard and M. Cutkosky. A design by composition approach for layered manufacturing. *ASME J Mechanical Design*, 122(1), 2000.

[9] B. Chan, N. J. Balmforth, and A. E. Hosoi. Building a better snail: Lubrication and gastropod locomotion. *Physics of Fluids*, 17, 2005.

[10] C.A. Dahlquist. Pressure-sensitive adhesives. In R.L. Patrick, editor, *Treatise on Adhesion and Adhesives*, volume 2, pages 219–260. Dekker, New York, 1969.

[11] K. Daltorio, S. Gorb, A. Peressadko, A. Horchler, R. Ritzmann, and R. Quinn. A robot that climbs walls using micro-structured polymer feet. In *CLAWAR*, 2005.

[12] K. Daltorio, A. Horchler, S. Gorb, R. Ritzmann, and R. Quinn. A small wall-walking robot with compliant, adhesive feet. In *International Conference on Intelligent Robots and Systems*, 2005.

[13] H. Gao, X. Wang, H. Yao, S. Gorb, and E. Arzt. Mechanics of hierarchical adhesion structures of geckos. *Mechanics of Materials*, 37:275–285, 2005.

[14] S. Gorb, M. Varenberg, A. Peressadko, and J. Tuma. Biomimetic mushroom-shaped fibrillar adhesive microstructure. *Journal of The Royal Society Interface*, 2006.

[15] K.L. Johnson, K. Kendall, and A.D. Roberts. Surface energy and the contact of elastic solids. *Proc. of the Royal Society A: Mathematical, Physical and Engineering Sciences*, 324(1558):301–313, 1971.

[16] K. Kendall. Thin-film peeling - the elastic term. *Journal of Physics D: Applied Physics*, 8(13):1449–1452, 1975.

[17] J. Kerr and B. Roth. Analysis of multifingered hands. *The International Journal of Robotics Research*, 4(4):3–17, 1986.

[18] D.S. Kim, H.S. Lee, J. Lee, S. Kim, K-H Lee, W. Moon, and T.H. Kwon. Replication of high-aspect-ratio nanopillar array for biomimetic gecko foot-hair prototype by uv nano embossing with anodic aluminum oxide mold. *Microsystem Technologies*, 2006.

[19] S. Kim and M. Sitti. Biologically inspired polymer microfibers with spatulate tips as repeatable fibrillar adhesives. *Applied Physics Letters*, 89(261911), 2006.

[20] S. Kim, M. Spenko, and M. Cutkosky. Whole body adhesion: hierarchical, directinoal and distributed control of adhesive forces for a climbing robot. In *IEEE ICRA*, Rome, Italy, 2007. Accepted.

[21] G. La Rosa, M. Messina, G. Muscato, and R. Sinatra. A lowcost lightweight climbing robot for the inspection of vertical surfaces. *Mechatronics*, 12(1):71–96, 2002.

[22] M. Northen and K. Turner. A batch fabricated biomimetic dry adhesive. *Nanotechnology*, 16:1159–1166, 2005.

[23] A. Peressadko and S.N. Gorb. When less is more: experimental evidence for tenacity enhancement by division of contact area. *Journal of Adhesion*, 80(4):247–261, 2004.

[24] D. Santos, S. Kim, M. Spenko, A. Parness, and M. Cutkosky. Directional adhesive structures for controlled climbing on smooth vertical surfaces. In *IEEE ICRA*, Rome, Italy, 2007. Accepted.

[25] A. Saunders, D. Goldman, R. Full, and M. Buehler. The rise climbing robot: body and leg design. In *SPIE Unmanned Systems Technology VII*, volume 6230, Orlando, FL, 2006.

[26] M. Sitti and R. Fearing. Synthetic gecko foot-hair micro/nano-structures as dry adhesives. *Adhesion Science and Technology*, 17(8):1055, 2003.

[27] O. Unver, M. Murphy, and M. Sitti. Geckobot and waalbot: Small-scale wall climbing robots. In *AIAA 5th Aviation, Technology, Integration, and Operations Conference*, 2005.

[28] vortex. www.vortexhc.com, 2006.

[29] L. E. Weiss, R. Merz, F. Prinz, G. Neplotnik, P. Padmanabhan, L. Schultz, and K. Ramaswami. Shape deposition manufacturing of heterogenous structures. *Journal of Manufacturing Systems*, 16(4):239–248, 1997.

[30] Z. Xu and P. Ma. A wall-climbing robot for labeling scale of oil tank's volume. *Robotica*, 20(2):203–207, 2002.

[31] H. Yao and H. Gao. Mechanics of robust and releasable adhesion in biology: Bottom-up designed hierarchical structures of gecko. *Journal of the mechanics and physics of solids*, 54:1120–1146, 2006.

[32] B. Yurdumakan, R. Raravikar, P. Ajayanb, and A. Dhinojwala. Syntheic gecko foot-hairs from multiwalled carbon nanotubes. *Chemical Communications*, 2005.

[33] Y. Zhao, T. Tong, L. Delzeit, A. Kashani, M. Meyyapan, and A. Majumdar. Interfacial energy and strength of multiwalled-carbon-nanotube-based dry adhesive. *Vacuum Science and Tech B*, 2006.

[34] J. Zhu, D. Sun, and S.K. Tso. Development of a tracked climbing robot. *Intelligent and Robotic Systems*, 35(4):427–444, 2002.